CMS data and their interpretation using the phenomenological MSSM

Maurizio Pierini

CERN

Maria Spiropulu

CERN & California Institute Of Technology, Pasadena

Filip Moortgat, Luc Pape

ETH, Zurich, Switzerland

Joseph Lykken

Fermi National Accelerator Laboratory, Batavia, Illinois

Harrison Prosper, Sezen Sekmen

Florida State University, Tallahassee

Sabine Kraml

LPSC, Grenoble

Sanjay Padhi

University of California, San Diego

Abstract

We interpret, for the first time, CMS data using the phenomenological MSSM (pMSSM). The pMSSM is a 19-parameter sub-model of the MSSM that encompasses a broad range of simpler—and therefore more constrained—SUSY models, including the CMSSM. Using profile likelihoods, we examine each of the 19 parameters separately, including a number of observables, and determine to which parameters the current CMS data are most sensitive. Our results, which are based on the 2010 CMS data-set corresponding to 35 pb^{-1} of integrated luminosity, provide new constraints on parameters sensitive to hadronic as well as multilepton final states. In contrast to the constraints provided by SUSY models such as the CMSSM, our constraints provided a more global view of what current data can say about the MSSM. While the focus of this note is the MSSM, the approach we describe is applicable to *any* multi-parameter model.

1 Introduction

With the extremely successful performence of both machine and detectors at $\sqrt{s} = 7$ TeV and good prospects to go soon into higher energies, the LHC is finally opening the window to the Terascale. Importantly, new insights are expected from the LHC data, most of all in the mechanism of electroweak (EW) symmetry breaking and, related to this, in the nature of new physics Beyond the Standard Model (BSM) stabilizing the EW scale.

A wealth of BSM theories has been put forth by the theoretical community and it is now up to experiments to test which, if any, of these theories are correct. The arguably best motivated, but certainly the best studied, such BSM theory is supersymmetry, SUSY for short. Indeed, searches for SUSY are among the primary objectives of the CMS collaboration. Here note that SUSY is exceedingly popular not only for its theoretical beauties but also because SUSY phenomenology is extremely rich, leading to a large variety of possible new signals at the LHC.

Over the years, it has become common practice to interpret collider results in terms of a strictly constrained parameterization of supersymmetry, namely the constrained minimal supersymmetric model (CMSSM). Though this setup has its practical implications, it lacks a sound theoretical motivation. In this work we would like to initiate an approach that uses a more generic, and theoretically more feasible expression of supersymmetry. We introduce here the phenomenological MSSM (pMSSM), studied recently by Berger et. al., which is a 19 parameter realization of SUSY defined at the SUSY scale $\sqrt{m_{\tilde{t}_1} m_{\tilde{t}_2}}$ as an acceptably generic scenario for interpreting the early LHC results of 35pb^{-1}. We use results from the dijet α_T analysis, the opposite-sign dilepton analysis and the same-sign dilepton analysis to see the effects of these early observations on our knowledge on pMSSM.

We start the note with giving the motivation to go beyond CMSSM and to work with pMSSM, which is followed by the definition and parameterization of pMSSM. We then outline our analysis, giving details on the pMSSM points we have used, the detector simulation and the CMS analyses, and later describe the statistical method based on profile likelihoods used for coping with the 19 dimensional setup of pMSSM. This is followed by the results and conclusion.

2 Motivation for a generic MSSM setup

The majority of SUSY studies related to the interpretation of collider data focus on a very special setup: the so-called Constrained Minimal Supersymmetric Standard Model (CMSSM). This was justified in the preparation for discoveries, as the CMSSM having just a handful of new parameters is very predicive. However, the simple assumption of universality at the GUT scale lacks a sound theoretical motivation; the CMSSM should hence be regarded as a showcase model. When it comes to interpreting experimental results, on the one hand it is reasonable and interesting to do this within the CMSSM, because it provides an easy way to show performances, compare limits or reaches, etc. On the other hand, as said above, SUSY phenomenology is extremely rich and by far not exploited by the $(m_0, m_{1/2})$ plane.

Indeed perhaps the least understood aspect of SUSY is its breaking, which in turn determines the boundary conditions for the Lagrange parameters at some high scale. Again, theorists have come up with a long list of possible candidate scenarios, including supergravity (SUGRA), gauge mediation (GMSB), anomaly mediation (AMSB), gaugino mediation, radion mediation, etc.. They come in minimal (mSUGRA, mGMSB, ...) and less minimal (e.g., non-universal Higgs masses, NUHM, or non-universal gaugino masses) variants, as well as in general setups (general gauge mediation, ...). Moreover, there are models of compressed or split SUSY, GUT-inspired models, string-inspired models, and so on. Each of these possibilities features characteristic relations between fundamental parameters and hence characteristic mass spectra, decay patterns and properties of the dark matter candidate.

The CMSSM covers just a subset of this spectrum. To give some examples:

- The CMSSM assumes universal gaugino masses $M_1 = M_2 = M_3 \equiv m_{1/2}$ at the GUT scale, leading to

$$M_1 : M_2 : M_3 \approx 1 : 2 : 7 \text{ with } M_1 \approx 0.4\, m_{1/2} \tag{1}$$

  at the EW scale, which is equivalent to $m_{\tilde{\chi}_2^0} \approx 2 m_{\tilde{\chi}_1^0} \approx 0.8\, m_{1/2}$ and $m_{\tilde{g}} \approx 7 m_{\tilde{\chi}_1^0} \approx 2.8\, m_{1/2}$. Other models can have very different relations between M_1, M_2, M_3, giving rise to the so-called "gaugino code" [1], which can be very useful for model discrimination. Besides, models with non-universal gaugino masses are quite natural [2] even within the SUGRA context, and they can have very low finetuning [3].

- Over most of the CMSSM parameter space $|\mu|^2 \gtrsim m_{1/2}^2$. The lightest neutralino is then mostly bino, the second-lightest mostly wino, and the heavier ones mostly higgsinos. Light higgsinos and large gaugino–higgsino mixing (mixed bino–higgsino dark matter) occur only in the focus point region, i.e. when squarks

and sleptons are very heavy. This has a strong impact on squark and gluino cascade decays, as well as on the part of parameter space that is compatible with dark matter constraints.

- Turning to the sfermion sector, the slepton-mass parameters are to good approximation

$$m_{\tilde{R}}^2 \approx m_0^2 + 0.15\, m_{1/2}^2\,, \qquad m_{\tilde{L}}^2 \approx m_0^2 + 0.5\, m_{1/2}^2\,. \tag{2}$$

Note that this implies that right-chiral states are alway lighter than the left-chiral ones. Combining Eqs. (1) and (2) we see that for small m_0 (but large enough to have a neutralino LSP) this leads to the typical mass pattern $m_{\tilde{\chi}_1^0} < m_{\tilde{e}_R} < m_{\tilde{\chi}_2^0} < m_{\tilde{e}_L}$. For the first two generations of squarks we have

$$m_{\tilde{U},\tilde{D}}^2 \approx m_0^2 + K m_{1/2}^2\,, \qquad m_{\tilde{Q}}^2 \approx m_0^2 + (K+0.5) m_{1/2}^2\,, \tag{3}$$

with $K \sim 4.5$ to 6.5, and the dependence on $m_{1/2}$ dominated by the gluino contribution, i.e. by M_3. It is clear that any limit on or determination of m_0 is completely dominated by the slepton sector [4]. Non-universal scalar masses are heavily constrained by flavour-changing neutral currents (FCNC), at least for the first and second generations. For the third generation, the FCNC constraints are much less severe. One possibility to motivate universal mass parameters for sfermions is to embed them in a higher gauge group, like SO(10). But even then, non-universalities can occur through D-term contributions [5] and/or GUT-scale threshold corrections [6, 7]. Besides, there is no sound theoretical motivation for unifying the mass-squared terms of the Higgs fields, $m_{H_1}^2$ and $m_{H_2}^2$, with those of the other scalars. If this is given up $m_{H_{1,2}}^2$, or equivalently μ and m_A, become free parameters of the model [8] (cf. the discussion of the value of μ above).

- The assumption of scalar mass universality has another important implication, namely that the renormalization-group invariant quantity

$$S = \left(m_{H_2}^2 + m_{H_1}^2\right) + \mathrm{Tr}\left(m_{\tilde{Q}}^2 - 2m_{\tilde{U}}^2 + m_{\tilde{D}}^2 + m_{\tilde{R}}^2 - m_{\tilde{L}}^2\right) \tag{4}$$

vanishes. This so-called S-parameter, if non-zero, influences the running of the scalar mass parametres M_ϕ^2 proportional to their hypercharge Y_ϕ

$$16\pi^2 \frac{d}{dt} M_\phi^2 = ... + \frac{6}{5} Y_\phi g_1^2 S\,. \tag{5}$$

This can change the mass ordering of left- and right-chiral states or have an important influence on the Higgs sector. In the CMSSM however $S \equiv 0$.

From these considerations, which are just exemplary and by no means complete, it is clear that it is interesting and necessary to go beyond the naïve CMSSM. We need to search for SUSY without prejudice [9, 10], even more so as we have all the necessary knowledge and machinery at our disposal. In this context note that major efforts have recently been devoted to developing precise statistical tools for analyzing new physics at the LHC [11]. This includes sophisticated methods and tools for the investigation of multi-dimensional parameter spaces, as typical for SUSY models. Below we therefore lay out a program for the investigation of the general minimal supersymmetric Standard Model, the so-called *phenomenological MSSM* (pMSSM), with 19 free parameters.

3 Phenomenological MSSM (pMSSM)

Phenomenological MSSM is a model that makes no assumptions on the SUSY breaking mechanism. It is parametrized at the so-called "SUSY scale (i.e. the geometric mean of the two stop masses). At this low scale, SUSY is defined by over 120 parameters at its most generic form. However simplifying assumptions can be made without loosing much from the generality of the scenario. pMSSM construction stays within the CP-conserving MSSM (i.e. no new phases) with minimal flavor violation. Moreover, to help soften the impact of experimental constraints arising from the flavor sector, the first two generations of sfermions are taken to be degenerate. This results in the following 19-dimensional parameterization:

1. 10 scalar masses: $m_{\tilde{f}}$ (where $\tilde{f} = \tilde{Q}_L, \tilde{Q}_3, \tilde{L}_1, \tilde{L}_3, \tilde{u}_1, \tilde{d}_1, \tilde{u}_3, \tilde{d}_3, \tilde{e}_1$, and $\tilde{e}_3$),
2. 3 gaugino masses: $M_{1,2,3}$ (pertaining to U(1), SU(2), and SU(3), respectively),
3. 1 $\tan\beta$ parameter,

4. 3 trilinear couplings: $A_{b,t,\tau}$,

5. 1 pseudo-scalar Higgs mass: m_A.

6. 1 μ parameter.

The parameters m_A and μ can be swapped for the Higgs mass parameters m_{H_u} and m_{H_d}.

Berger et. al. performed a multi-dimensional scan to find out what regions in the pMSSM parameter space are consistent with theoretical and experimental constrains. They did a uniform random sampling of points from within the pMSSM subspace defined by the parameter ranges below

$$\begin{aligned} 100 \text{ GeV} \leq \quad & m_{\tilde{f}} & \leq 1000 \text{ GeV}, \\ 50 \text{ GeV} \leq \quad & |M_{1,2}, \mu| & \leq 1000 \text{ GeV}, \\ 100 \text{ GeV} \leq \quad & M_3 & \leq 1000 \text{ GeV}, \\ & |A_{b,t,\tau}| & \leq 1000 \text{ GeV}, \\ 1 \leq \quad & \tan\beta & \leq 50, \\ 43.5 \text{ GeV} \leq \quad & m_A & \leq 1000 \text{ GeV}, \end{aligned} \tag{6}$$

4 Current experimental and theoretical constraints

The most relevant constraints today are the [SUSY and Higgs] mass limits from LEP2 and the Tevatron, electroweak precision observables, the branching ratios of the decays $B \to X_s\gamma$ and $B_s \to \mu^+\mu^-$, the anomalous magnetic moment of the muon $(g-2)_\mu$, and the relic density of dark matter Ωh^2. They are compiled in Table 1 (to be extended).

Other important constraints, which we are not yet taking into account, come from m_W, $A_b^{\rm FB}$ and ΔM_b.

Observable	exp. constraint	ref.	add. theory error	ref.
M_Z [GeV]	91.1875 ± 0.0021	[12]	–	
M_t [GeV]	173.3 ± 1.1	[13]	–	
$m_b(m_b)^{\overline{\rm MS}}$ [GeV]	$4.19^{+0.18}_{-0.06}$	[12]	–	
$\alpha_s(M_Z)^{\overline{\rm MS}}$	0.1184 ± 0.0007	[12]	–	
	or 0.1176 ± 0.002	[12]	–	
m_h [GeV]	≥ 114.4	[14]	± 1.5	[15]
$\Delta a_\mu \times 10^{-10}$	e^+e^- : 29.6 ± 8.1	[16]	± 2	
	$\tau's$: 15.7 ± 8.2	[**?**]		
$\text{BR}(b \to s\gamma) \times 10^{-4}$	$3.55 \pm 0.24_{\rm stat} \pm 0.09_{\rm sys}$	[17]	?	
$\text{BR}(B_s \to \mu^+\mu^-)$	$\leq 3.6 \times 10^{-8}$	[17]	?	
$\Omega_{\rm DM} h^2$	0.1123 ± 0.0035	[18]	?	
SUSY masses	LEP2 limits	[19]	?	

Table 1: Important observables, to be used in the likelihood calculation.

5 Analysis

The goal of this study is to determine whether current CMS data are sufficient to impose visible constraints on the pMSSM parameter space, and consequently on SUSY mass scales and low energy observables such as $(g-2)_\mu$, BR($b \to s\gamma$), etc. To achieve this goal, we carry out the following analysis steps:

- For each of the 6K pMSSM points we generate 10K events.
- We perform three approved CMS analyses, namely the "di-jet α_T" (Had), "opposite-sign di-lepton" (OS) and "same-sign di-lepton" (SS) analyses on each of the 6K pMSSM samples.
- For each pMSSM point and for each of the three analyses, we combine the predicted signal yield s with the approved CMS results—the observed event count N and a data-driven background estimate $b \pm \delta b$—to compute the likelihood as a function of the pMSSM parameters.

- We weight every pMSSM point with the product of the three likelihoods, one for each of the three analyses. Since the pMSSM points were sampled from a (bounded) uniform 19-dimensional density, the set of weights constitute a non-parametric representation of the likelihood function.
- In order to illustrate the contribution of the current CMS data, we calculate profile likelihoods for the relevant model parameters, with and without the CMS likelihood, that is, the weights.

5.1 Event samples

We use a 6K subset of the pMSSM points generated by Berger *et al.* as explained in Section **??**. Information on each point is contained in a SUSY Les Houches (SLHA) [20] file. For each point, 10K events were generated using `PYTHIA6` [21]. We simulate the response of the CMS detector using the publicly available general purpose detector simulation package `Delphes` [22]. Through extensive numerical and shape comparisons we conclude that we are able to provide a *very* fast simulation of the CMS detector that is good to within 10%. An accurate, fast, simulation is critical for studies of this scope.

5.2 Implementation of the three approved CMS analyses

Table 2: Comparison of signal Monte Carlo yields for the 3 CMS analyses

	LM0		LM1	
	CMSSW	Delphes	CMSSW	Delphes
Dijet α_T				
OS di-lepton				
SS dil-epton				

Table 3: Numerical results of the three CMS analyses for 35 pb^{-1} as given by `CMSSW` full simulation and `Delphes` for the SUSY benchmarks LM0 and LM1.

Analysis (k)	Observed data count (N_k)	Data-driven SM BG estimate ($b_k \pm \delta b_k$)	MC SM BG prediction ($b_k^{MC} \pm b_k^{MC}$)
Dijet α_T	14	11.4 ± 2.0	9.2 ± 0.9
OS di-lepton	1	2.1 ± 2.1	1.27
SS di-lepton	0	1.2 ± 0.8	0.35

5.3 Calculation of the likelihood function

Every analysis k yields an observed count N_k and a background estimate $b_k \pm \delta b_k$ where $k = 1, 2, 3$. We make the standard assumption that the counts are Poisson distributed in which case the total likelihood from the combination of the three analyses can be written as

$$L(\theta) \equiv p(N|s,b) = \prod_{k=1}^{3} \text{Poisson}(N_k|s_k + b_k), \tag{7}$$

where s_k is the predicted signal and $L(\theta)$ the likelihood written as a function of the d =19-dimensional pMSSM parameter θ. In this study, the map of θ to the expected signals s_k is represented non-parametrically using the 6K pMSSM points. In principle, we could build a smooth functional approximation to this map; however, we have not attempted this in the current study. The likelihood values $L(\theta_i)$, where i is the ith pMSSM point, is used as the weight for this point. This is how we incorporate the likelihood function of the three approved CMS analyses in our pMSSM interpretation of the CMS results.

For any likelihood function, exact confidence regions [**?**] can *always* be created in the unrestricted parameter space. However, such confidence regions are seldom useful when the dimensionality of the parameter space is large. It is more useful to examine parameters one or two at a time. In the current study, we examine each parameter separately using the profile likelihood, a broadly applicable frequentist construct.

5.4 Calculation of profile likelihoods

As noted above, an important goal of this study is to determine to which pMSSM parameters the current CMS dataset is most sensitive and to what degree. This is useful because we shall be able to make statements whose validity is much broader than those made using models in which strong, but weakly motivated, simplifying assumptions have been made. A well-established way of conveying relevant information about the parameters of interest is to display their 1-dimensional profile likelihoods. We do this for each pMSSM parameter as well as for some observables.

Suppose we wish to investigate the gluino mass parameter M_3. Its (1-dimensional) profile likelihood, L_p, [?] is defined by

$$L_p(M_3) \equiv L(M_3, \hat{\theta}_2(M_3), \cdots, \hat{\theta}_{19}(M_3)), \tag{8}$$

where $\hat{\theta}_2 \cdots \hat{\theta}_{19}$ denote the maximum likelihood estimates (MLE), for a given value of M_3, of the remaining 18 parameters. Since we do not have a functional approximation of the map from θ to the expected signals, our likelihood function $L(\theta)$ is available non-parametrically as a swarm of weighted points, so standard maximizing programs such as `MINUIT` cannot be used. We have therefore devised our own non-parametric profiling algorithm, which proceeds as follows:

1. For each 1-dimensional bin of the parameter or observable of interest, for example M_3, we create a d-dimensional histogram of the 6K points using the Root class `TKDTreeBinning`. Through recursive binary partitioning, this class creates d-dimensional bins with equal bin content.
2. For a given bin, e.g. in the gluino mass parameter M_3, we find which of the 6K points is consistent with the given value of M_3.
3. Using these points, we find the bin with the maximum density (the one with the smallest volume) and use that as an estimate of the profile likelihood value for the given value of M_3.
4. In addition, in order to provide a better estimate, the above procedure is repeated 100 times, each with a different bootstrap sample of the original 6K points and the average is taken over the profiles in each bin. This in turn is done for each of the ~ 70 variables under investigation.

6 Results

7 Conclusion

We have studied

Acknowledgements

We thank JoAnne Hewett and Thomas G. Rizzo for providing us the 6K pMSSM points used in this analysis.

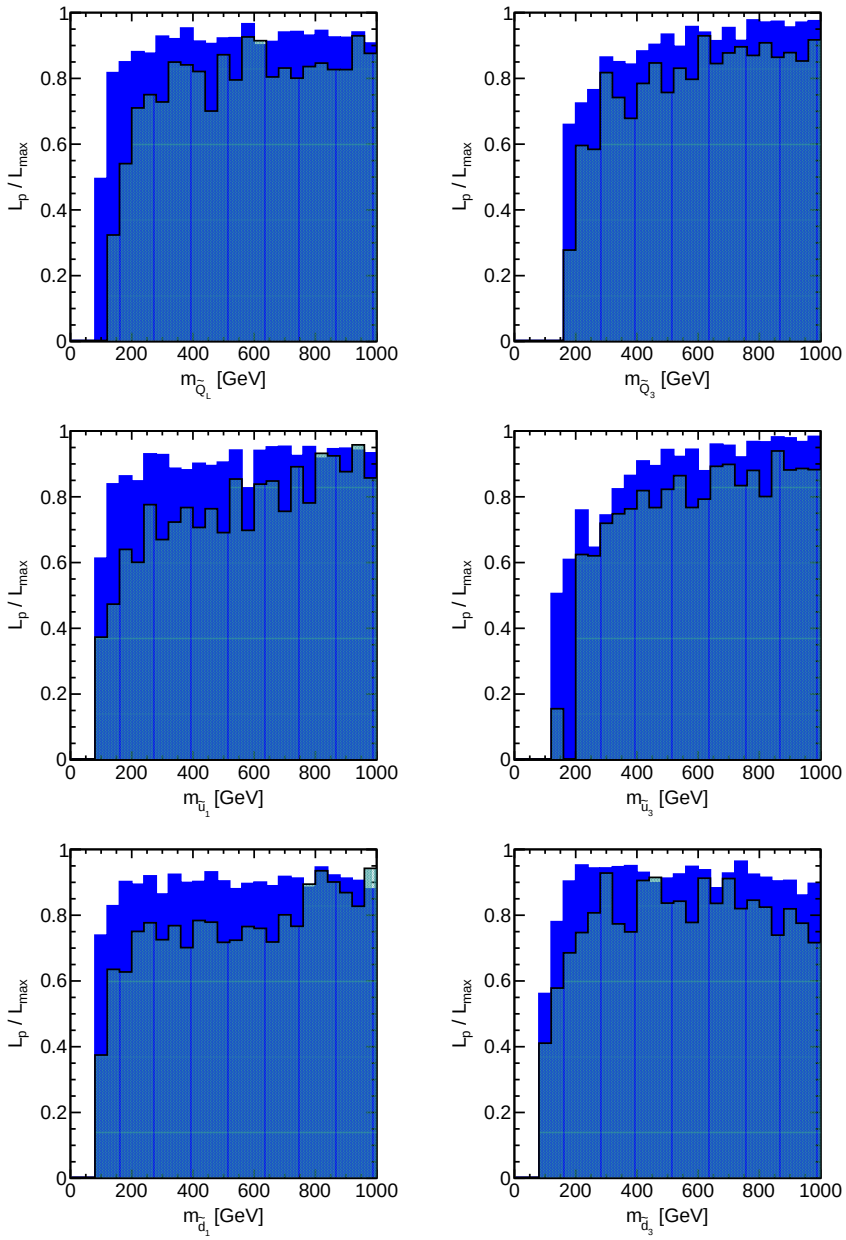

Figure 1: Ratios of profile likelihood L_p to maximum likelihood L_{max} shown for the squark mass parameters at SUSY scale. The colored and shaded histograms show the distributions before and after the inclusion of the CMS results.

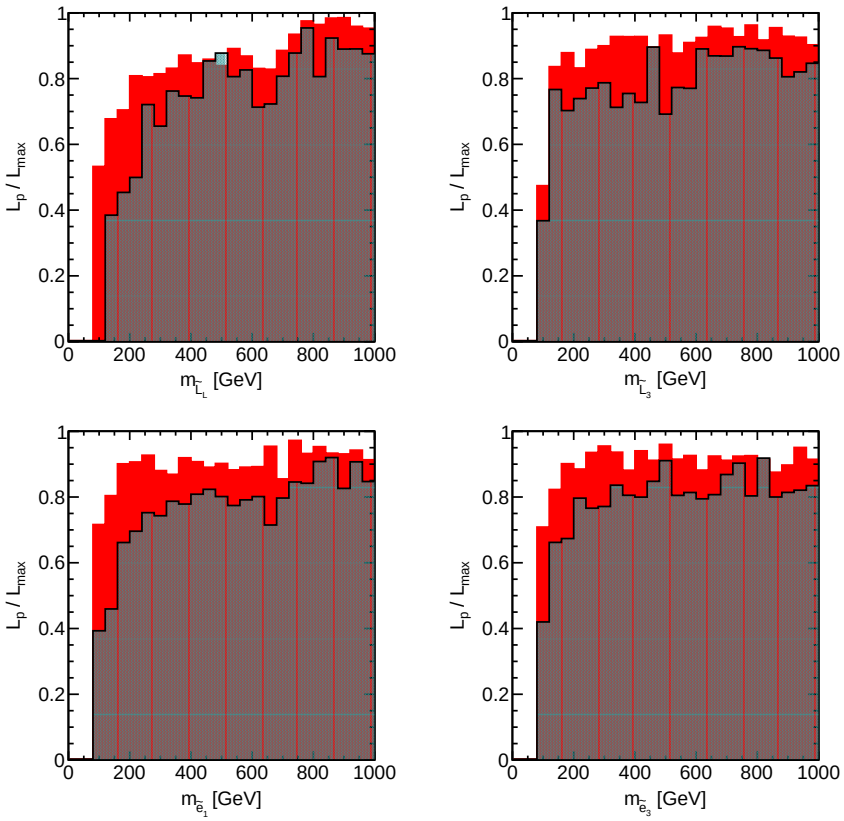

Figure 2: Ratios of profile likelihood L_p to maximum likelihood L_{max} shown for the slepton mass parameters at SUSY scale. The colored and shaded histograms show the distributions before and after the inclusion of the CMS results.

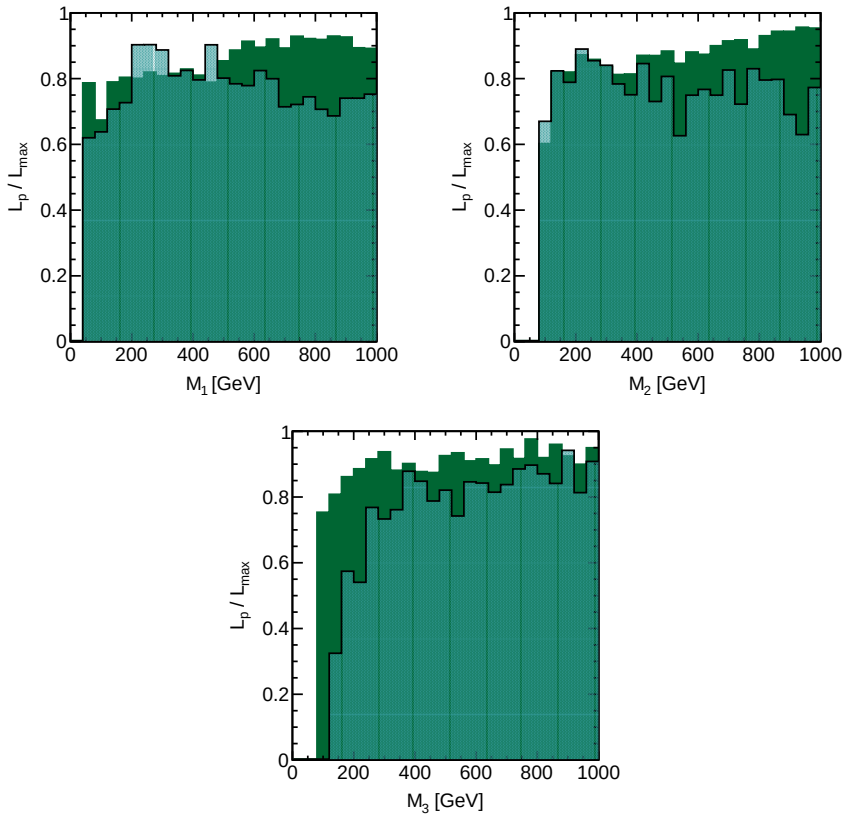

Figure 3: Ratios of profile likelihood L_p to maximum likelihood L_{max} shown for gaugino mass parameters at SUSY scale. The colored and shaded histograms show the distributions before and after the inclusion of the CMS results.

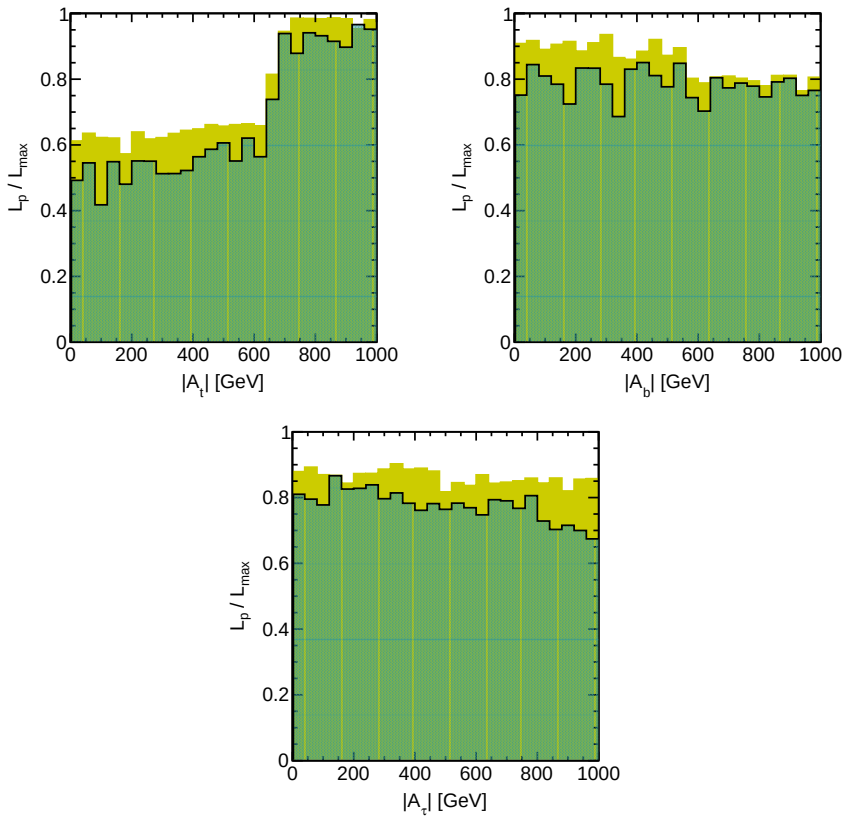

Figure 4: Ratios of profile likelihood L_p to maximum likelihood L_{max} shown for trilinear couplings at SUSY scale. The colored and shaded histograms show the distributions before and after the inclusion of the CMS results.

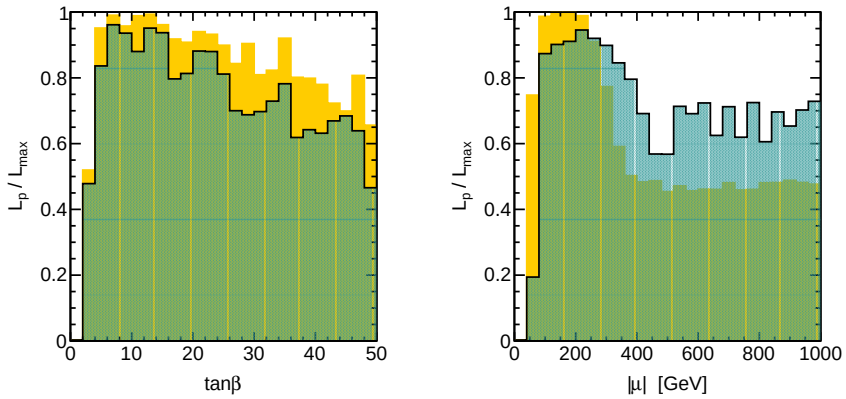

Figure 5: Ratios of profile likelihood L_p to maximum likelihood L_{max} shown for $\tan\beta$ and μ parameter at SUSY scale. The colored and shaded histograms show the distributions before and after the inclusion of the CMS results.

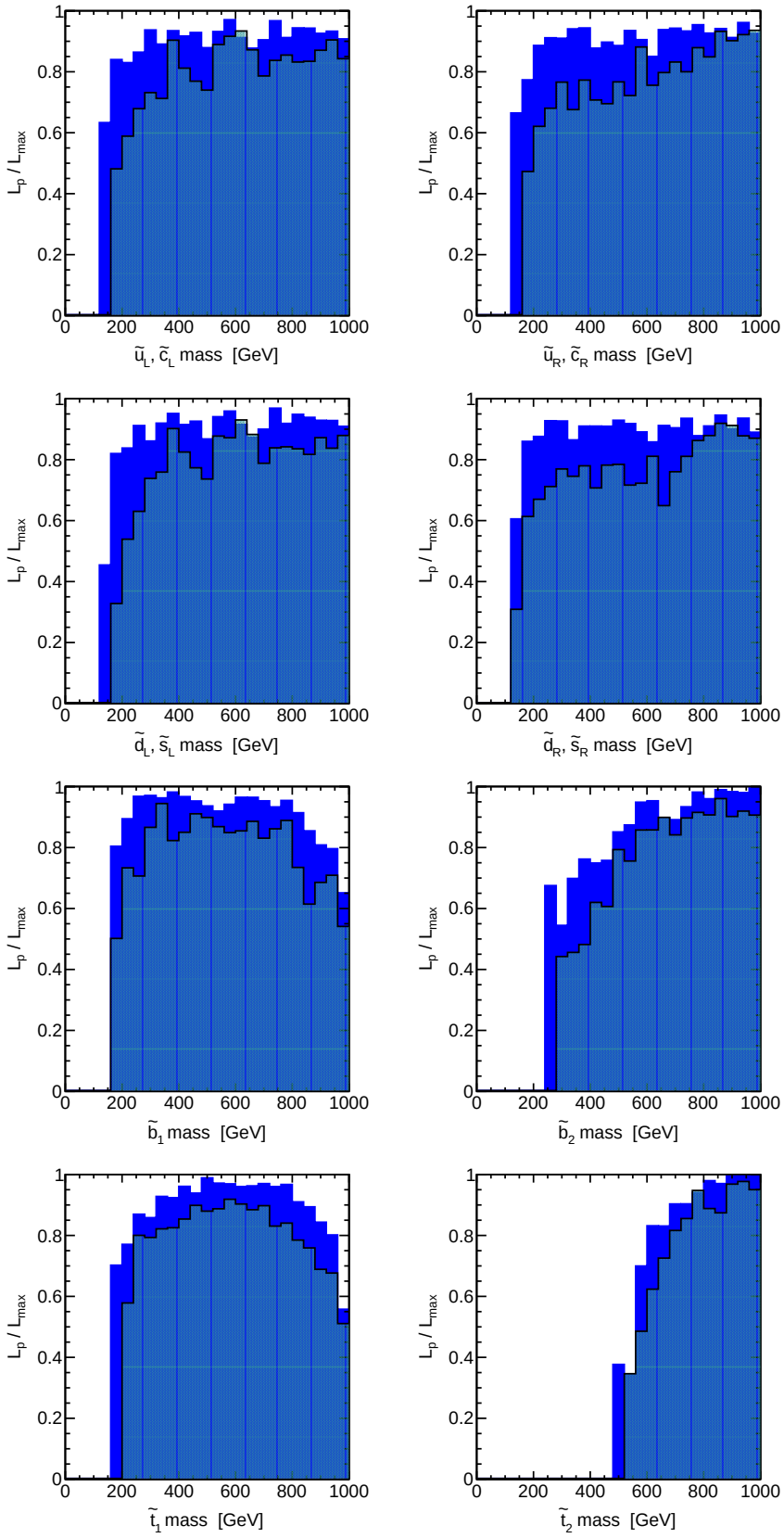

Figure 6: Ratios of profile likelihood L_p to maximum likelihood L_{max} shown for squark masses. The colored and shaded histograms show the distributions before and after the inclusion of the CMS results.

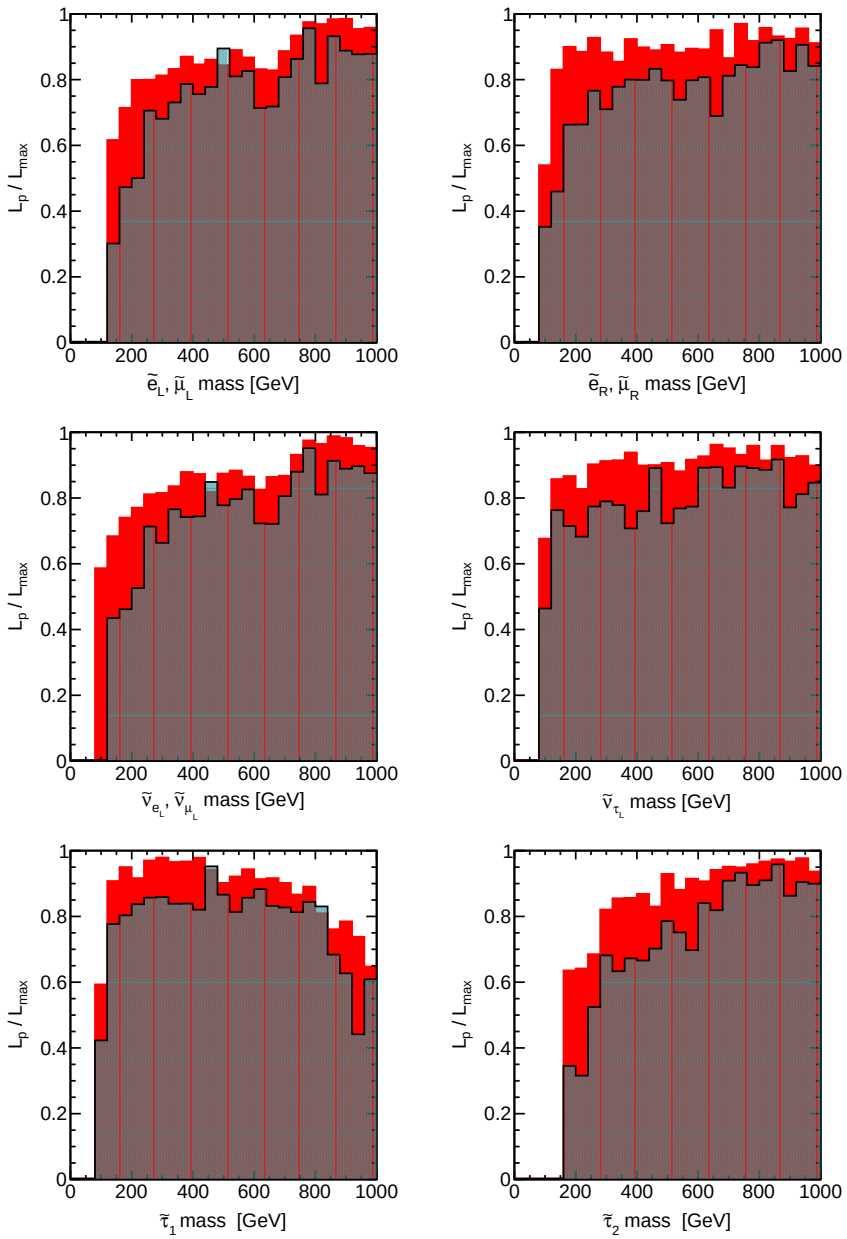

Figure 7: Ratios of profile likelihood L_p to maximum likelihood L_{max} shown for predictions for slepton masses. The colored and shaded histograms show the distributions before and after the inclusion of the CMS results.

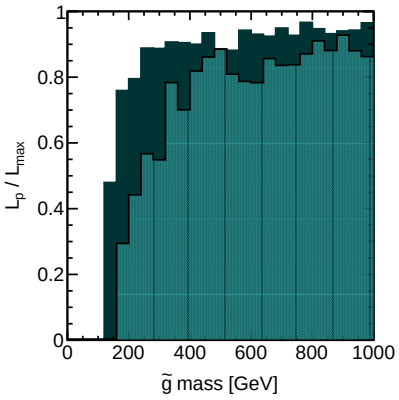

Figure 8: Ratios of profile likelihood L_p to maximum likelihood L_{max} shown for the gluino mass. The colored and shaded histograms show the distributions before and after the inclusion of the CMS results.

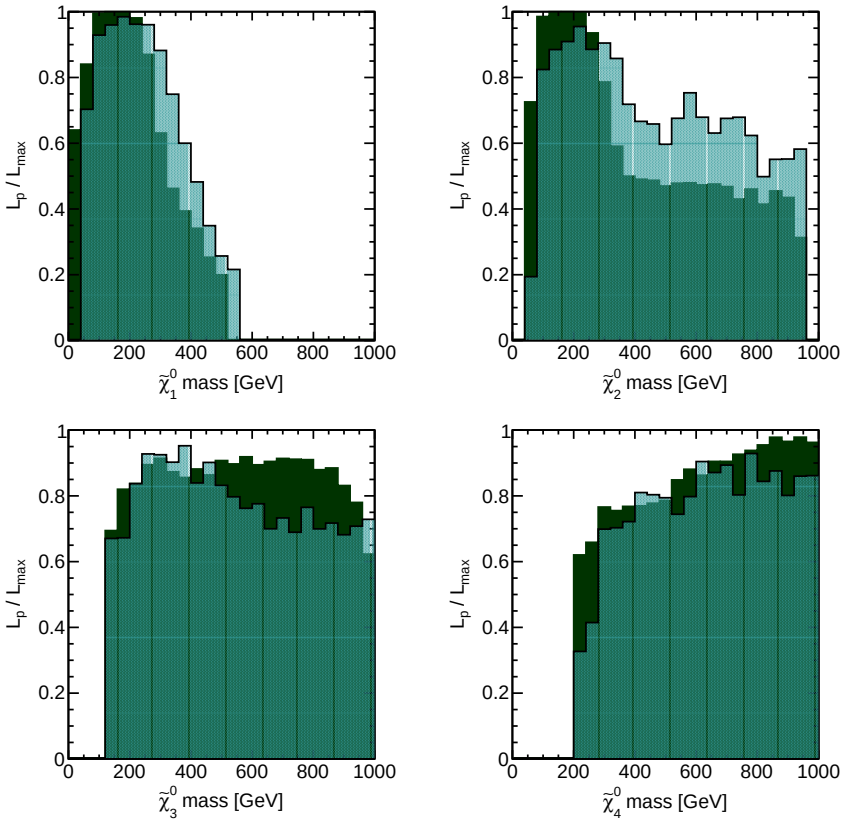

Figure 9: Ratios of profile likelihood L_p to maximum likelihood L_{max} shown for the neutralino masses. The colored and shaded histograms show the distributions before and after the inclusion of the CMS results.

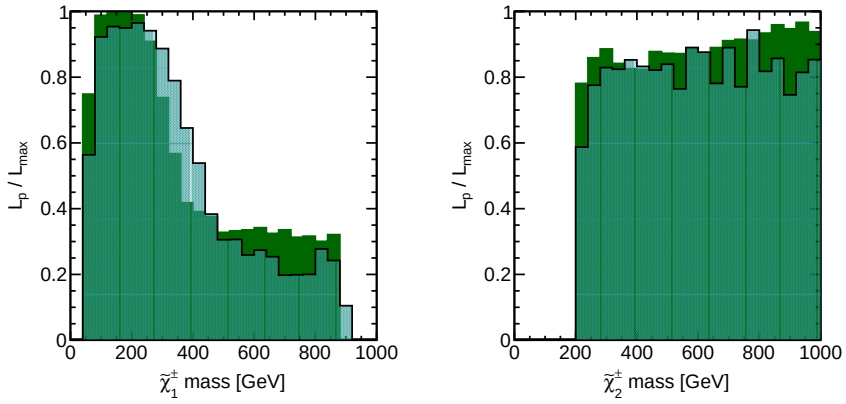

Figure 10: Ratios of profile likelihood L_p to maximum likelihood L_{max} shown for chargino masses. The colored and shaded histograms show the distributions before and after the inclusion of the CMS results.

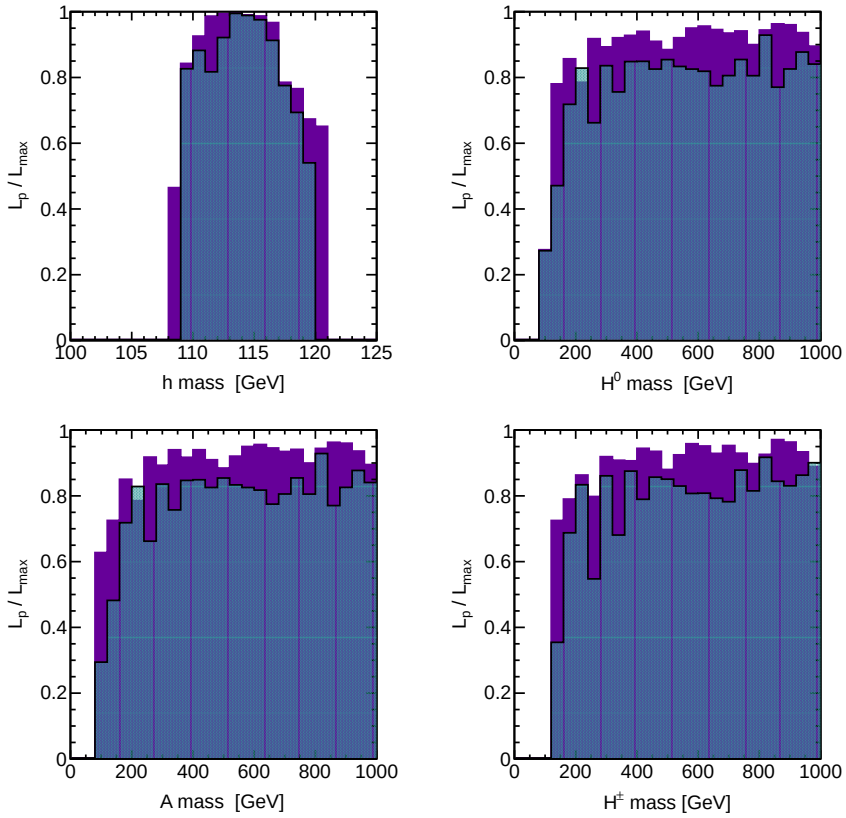

Figure 11: Ratios of profile likelihood L_p to maximum likelihood L_{max} shown for the Higgs masses. The colored and shaded histograms show the distributions before and after the inclusion of the CMS results.

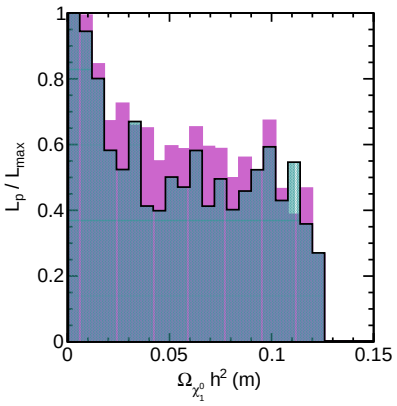

Figure 12: Ratio of profile likelihood L_p to maximum likelihood L_{max} shown for lightest neutralino dark matter relic density. The colored and shaded histograms show the distributions before and after the inclusion of the CMS results.

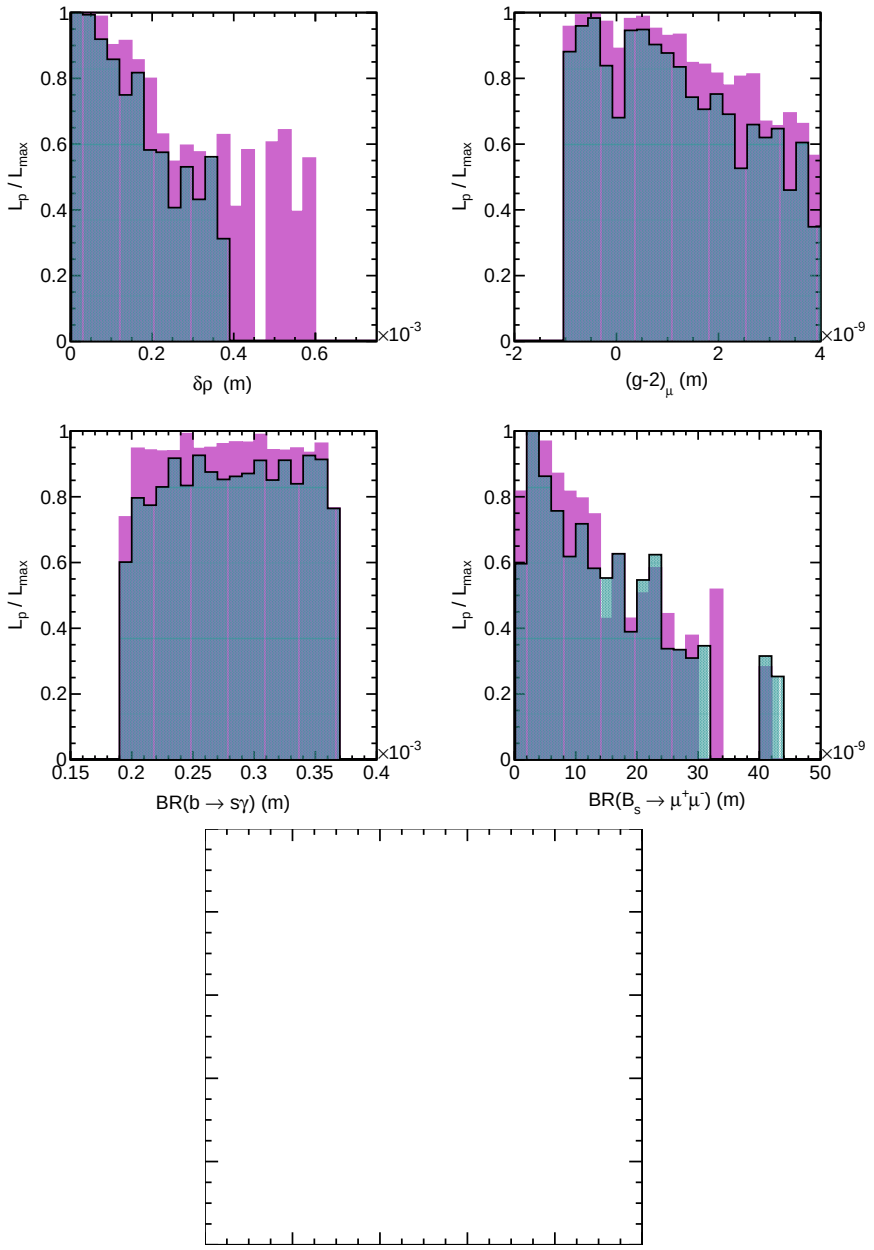

Figure 13: Ratios of profile likelihood L_p to maximum likelihood L_{max} shown for predictions for weak scale observables as calculated by micromegas. The colored and shaded histograms show the distributions before and after the inclusion of the CMS results.

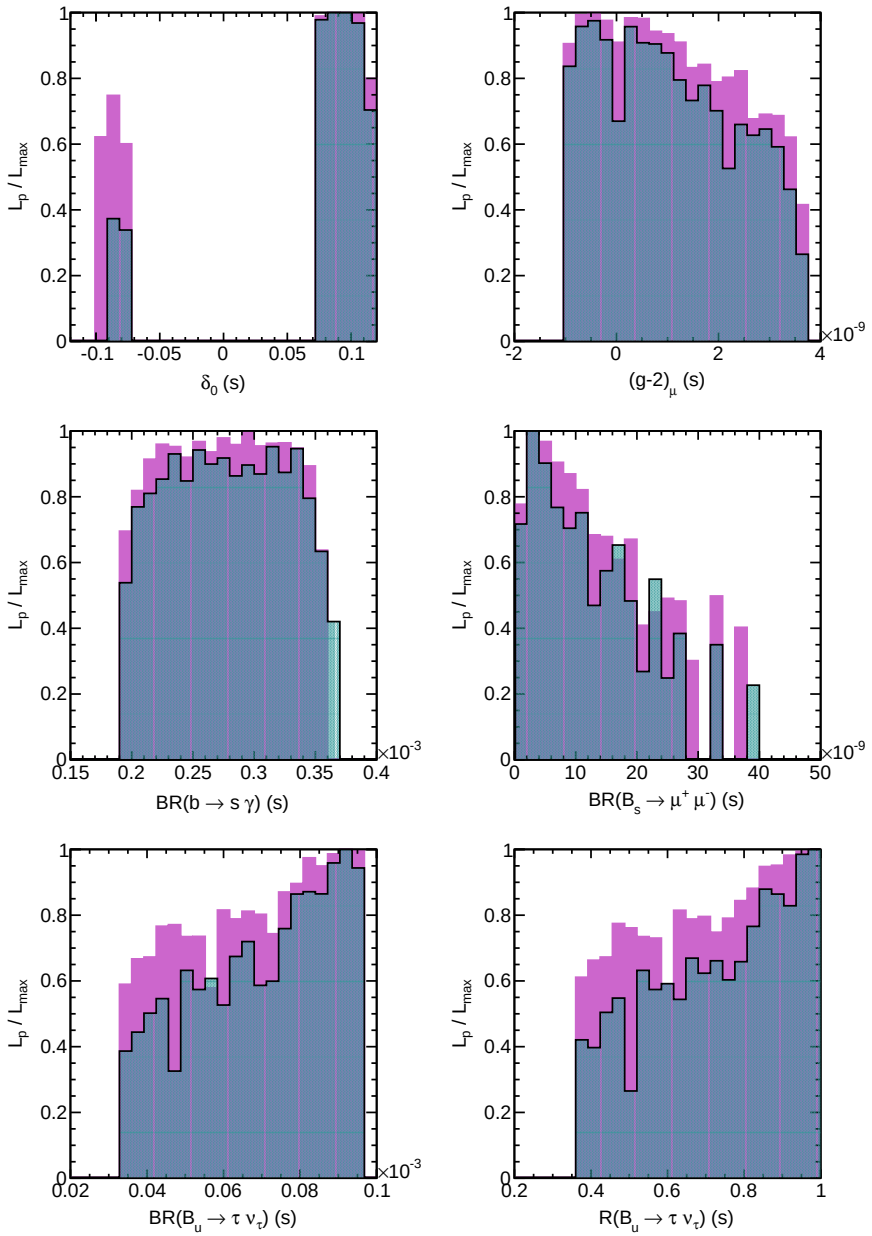

Figure 14: Ratios of profile likelihood L_p to maximum likelihood L_{max} shown for predictions for weak scale observables as calculated by superiso - I. The colored and shaded histograms show the distributions before and after the inclusion of the CMS results.

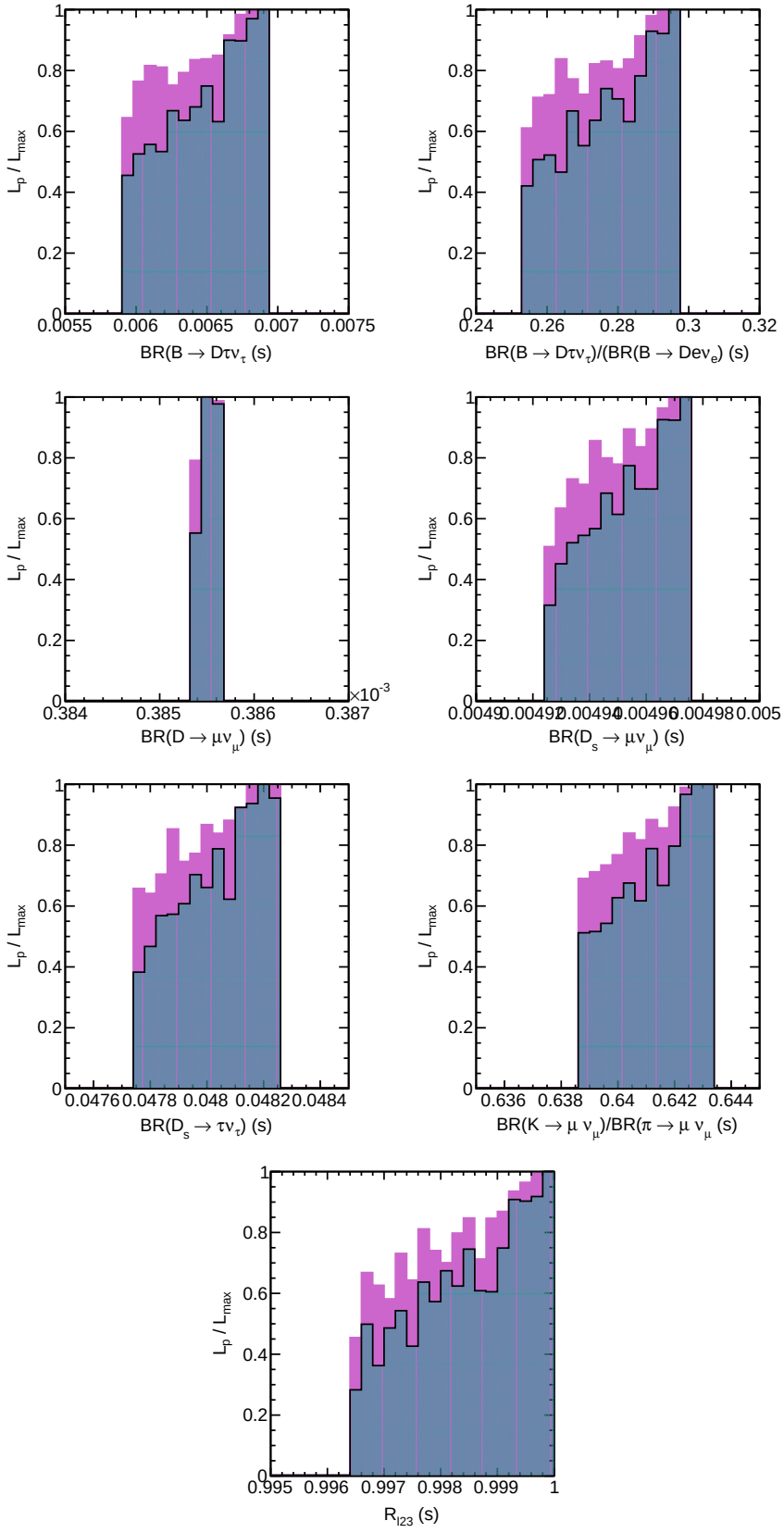

Figure 15: Ratios of profile likelihood L_p to maximum likelihood L_{max} shown for predictions for weak scale observables as calculated by superiso - II. The colored and shaded histograms show the distributions before and after the inclusion of the CMS results.

Appendix

We describe the (frequentist) statistical procedures we have used in this study. Suppose that our goal is to make a statement about the parameter θ_1, say the gluino mass parameter M_3, independently of the remaining 18 pMSSM parameters. Since the expected signal s is a function of $d = 19$ parameters (see Sect. (**??**), which we denote by $\theta = \theta_1, \cdots, \theta_{19}$, we need to eliminate $d - 1$ of them from the likelihood function so that the latter becomes a function of θ_1 only. In general, it is extremely difficult to do this in a frequentist calculation in a way that preserves *exact* coverage over the entire parameter space. However, let $L_p(\theta_1) \equiv L(\theta_1, \hat{\theta}_2(\theta_1), \cdots)$ be the 1-dimensional *profile likelihood*, that is, the function obtained by maximizing the likelihood function $L(\theta_1, \theta_2, \cdots, \theta_{19})$ with respect to $\theta_2, \cdots, \theta_{19}$ for *fixed* θ_1 and replacing the exact, but unknown, values of $\theta_2, \cdots, \theta_{19}$ by their maximum likelihood estimates (MLE), $\hat{\theta}_2(\theta_1), \cdots, \hat{\theta}_{19}(\theta_1)$.

Replacing exact values by estimates is clearly an approximation. We should therefore not expect any procedure that uses this approximation to yield confidence limits and intervals with exact coverage. However, in practice, 1-dimensional profile likelihoods created from multi-parameter likelihood functions often perform surprisingly well [?]. Let L_{max} be the maximum of the likelihood function $L(\theta)$ and let $\Lambda = L_p/L_{max}$ be the likelihood ratio. If the partial derivatives with respect to θ_i of the likelihood function, $L(\theta)$, exist up to second order and they form a $d \times d$ non-singular matrix (the Hessian), the following result holds,

$$W = -2 \log \Lambda \rightarrow \chi^2, \tag{9}$$

as the amount of data grows without limit. This is Wilks theorem [**?**, ?]. For an approximate 95% C.L. lower limit on θ_1, we set $W = 1.64$, that is, $\Lambda = 0.44$, and solve for the lower limit.

Non-parametric profiling algorithm

The problem we need to solve is the following: for a fixed value of a parameter, say Q, we want to find the maximum value of the likelihood function when the latter is available only as a weighted swarm of points. The quantity Q could be a pMSSM parameter, a predicted observable of a sparticle mass. Here, written as pseudo-code, is our algorithm for finding the profile likelihood:

```
1 pMSSMPOINTS, QBIN, Q = inputs()
2 NBOOTSTRAP = 100
3 profile = 0

4 repeat NBOOTSTRAP times:

5       POINTS = generateBootstrapSample(pMSSMPOINTS)
6       histogram = histogramPoints(POINTS)

7       DMAX = -1
8       for point in POINTS:

9            if Q not in QBIN: continue

10            d = histogram.density(point)
11            if d > DMAX: DMAX = d

12       profile = profile + DMAX

13  profile = profile / NBOOTSTRAP
14  return profile
```

1 Get the pMSSM points, the bin $QBIN$ for which the profile likelihood is to be computed, and the value of Q.

6 Generate a d-dimensional histogram from current bootstrap sample.

9 Make sure Q lies in desired bin $QBIN$.

10,11 Find largest density $DMAX$ so far.

12–14 Return average of estimates of profile likelihood.

The above algorithm is implemented in a class we developed called `KDTProfileLikelihood`, which makes use of the multi-dimensional histogrammer `TKDTreeBinning` in Root. The d-dimensional histogram is created through recursive binary partitioning of the parameter space in such a way that bins have equal counts. The underlying data structure is a kd-tree [**?**].

References

[1] K. Choi and H. P. Nilles, JHEP **04**, 006 (2007), hep-ph/0702146.

[2] S. P. Martin, Phys. Rev. **D79**, 095019 (2009), 0903.3568.

[3] D. Horton and G. G. Ross, Nucl. Phys. **B830**, 221 (2010), 0908.0857.

[4] B. C. Allanach *et al.*, (2006), hep-ph/0602198.

[5] C. F. Kolda and S. P. Martin, Phys. Rev. **D53**, 3871 (1996), hep-ph/9503445.

[6] N. Polonsky and A. Pomarol, Phys. Rev. Lett. **73**, 2292 (1994), hep-ph/9406224.

[7] N. Polonsky and A. Pomarol, Phys. Rev. **D51**, 6532 (1995), hep-ph/9410231.

[8] J. R. Ellis, K. A. Olive, and Y. Santoso, Phys. Lett. **B539**, 107 (2002), hep-ph/0204192.

[9] C. F. Berger, J. S. Gainer, J. L. Hewett, and T. G. Rizzo, JHEP **02**, 023 (2009), 0812.0980.

[10] J. A. Conley, J. S. Gainer, J. L. Hewett, M. P. Le, and T. G. Rizzo, (2010), 1009.2539.

[11] L. Lyons, (ed.), R. P. Mount, (ed.), and R. Reitmeyer, (ed.), Prepared for PHYSTAT2003: Statistical Problems in Particle Physics, Astrophysics, and Cosmology, Menlo Park, California, 8-11 Sep 2003.

[12] Particle Data Group, K. Nakamura, J. Phys. **G37**, 075021 (2010).

[13] CDF and D0, and others, (2010), 1007.3178.

[14] ALEPH, DELPHI, L3 and OPAL collaborations and the LEP Working Group for Higgs Boson Searches, S. Schael *et al.*, Eur. Phys. J. **C47**, 547 (2006), hep-ex/0602042.

[15] G. Degrassi, S. Heinemeyer, W. Hollik, P. Slavich, and G. Weiglein, Eur. Phys. J. **C28**, 133 (2003), hep-ph/0212020.

[16] M. Davier, A. Hoecker, B. Malaescu, and Z. Zhang, (2010), 1010.4180.

[17] The Heavy Flavor Averaging Group, D. Asner *et al.*, (2010), 1010.1589.

[18] N. Jarosik *et al.*, (2010), 1001.4744.

[19] ALEPH, DELPHI, L3 and OPAL, LEP2 SUSY Working Group,, `http://lepsusy.web.cern.ch/lepsusy/`.

[20] P. Z. Skands *et al.*, JHEP **0407** (2004) 036 [arXiv:hep-ph/0311123].

[21] T. Sjostrand, S. Mrenna and P. Z. Skands, JHEP **0605** (2006) 026 [arXiv:hep-ph/0603175].

[22] S. Ovyn, X. Rouby and V. Lemaitre, arXiv:0903.2225 [hep-ph].

[23] G. Belanger, F. Boudjema, A. Pukhov and A. Semenov, Comput. Phys. Commun. **176**, 367 (2007) [arXiv:hep-ph/0607059].

[24] F. Mahmoudi, Comput. Phys. Commun. **180**, 1579 (2009) [arXiv:0808.3144 [hep-ph]].